
In vitro bioactivity of S520 glass fibers and initial assessment of osteoblast attachment

D. C. Clupper,¹ J. E. Gough,¹ M. M. Hall,² A. G. Clare,² W. C. LaCourse,² L. L. Hench¹

¹Centre for Tissue Engineering, Materials Department, Imperial College of Science, Technology, and Medicine, Prince Consort Road, London, SW7 2BP, United Kingdom

²Department of Ceramic Engineering and Materials Science, Alfred University, Alfred, New York 14802

Received 4 February 2002; revised 25 October 2002; accepted 9 January 2003

Abstract: Bioactive glass fibers are attractive materials for use as tissue-engineering scaffolds and as the reinforcing phase for resorbable bioactive composites. The bioactivity of S520 glass fibers (52.0 mol % SiO₂, 20.9 Na₂O, 7.1 K₂O, 18.0 CaO, and 2.0 P₂O₅) was evaluated in two media, simulated body fluid (SBF) and Dulbecco's modified Eagle's medium (DMEM), for up to 20 days at 37°C. Hydroxyapatite formation was observed on S520 fiber surfaces after 5 h in SBF. After a 20-day immersion, a continuous hydroxyapatite layer was present on the surface of samples immersed in SBF as well as on those samples immersed in DMEM [fiber surface area to solution volume ratio (SA:V) of 0.10 cm²/mL]. Backscattered electron imaging and EDS analysis revealed that the hydroxyapatite layer formation was more extensive for samples immersed in SBF. Decreasing the SA:V ratio to 0.05 cm²/mL decreased the time required to form a continuous hydroxyapatite surface layer. ICP was used to reveal Si, Ca, and P release profiles in DMEM after the 1st h

(15.1, 83.8, and 29.7 ppm, respectively) were similar to those concentrations previously determined to stimulate gene expression in osteoblasts *in vitro* (16.5, 83.3, and 30.4 ppm, respectively). The tensile strength of the 20- μ m diameter fibers was 925 \pm 424 MPa. Primary human osteoblast attachment to the fiber surface was studied by using SEM, and mineralization was studied by using alizarin red staining. Osteoblast dorsal ruffles, cell projections, and lamellipodia were observed, and by 7 days, cells had proliferated to form monolayer areas as shown by SEM. At 14 days, nodule formation was observed, and these nodules stained positive for alizarin red, demonstrating Ca deposition and, therefore mineralization. © 2003 Wiley Periodicals, Inc. *J Biomed Mater Res 67A*: 285–294, 2003

Key words: glass fibers; bioactivity; hydroxyapatite; cell attachment; mineralization

INTRODUCTION

One of the primary goals in the field of tissue engineering is the development of scaffold materials that support, stimulate, and direct the growth of specific cells undergoing collective processes that ultimately lead to the creation of a specific tissue type. The selection of a proper material for the scaffold is of course a concern, but the geometrical architecture of the scaffold is important as well. Porous foams¹ and fibrous meshes^{2,3} are common motifs, because the interconnected nature of such designs allows for the diffusion of cell nutrients and the ingrowth of vascular tissue.

Bioactive glasses are potential candidates for use in the construction of tissue-engineering scaffolds. Several compositions of bioactive glass (and glass-ceramics) have that are able to form bonelike hydroxyapatite

surface layers when immersed in buffered fluids with ionic concentrations similar to those found in human blood plasma have been discovered.^{4–6} The presence of hydroxyapatite on the surface of bioactive glasses or glass-ceramics may encourage osteoconduction and bone bonding.^{7,8} The specific biological mechanisms that contribute to this property have been a matter of speculation for some time, but recent studies have indicated that the ionic dissolution products of the bioactive glass 45S5 stimulate the upregulation of a host of genes that lead to differentiation of osteoprogenitor cells. In effect, the bioactive glass is capable of “turning on” genetic information in such a way that the production of bone-building cells is enhanced.⁹ This finding suggests that bioactive glass could be a useful component in a scaffold designed to support and stimulate the formation of calcified tissue.

A new glass, designated as S520, that can easily be converted into fiber by using a continuous draw process has been developed.¹⁰ The primary features of the S520 composition are an elevated silica content and

Correspondence to: D. Clupper; e-mail: clupper@bellsouth.net

the replacement of a portion of soda with potassia to take advantage of the mixed alkali effect. As a result, devitrification of the glass is greatly inhibited and fragility is reduced, which aids the fiber-forming process.

Preliminary reactivity testing in a simple Tris-HCl buffering solution indicated that S520 glass fibers reacted to form a surface hydroxyapatite layer.¹⁰ Therefore, it was concluded that the S520 composition was nominally bioactive. However, the actual environment under which such a fiber would function is more complex. The culturing media, which provide nourishment to cells used in tissue-engineering applications, are generally rich in inorganic ions and organic species such as basic carbohydrates and amino acids. Therefore, additional meaningful information about the S520 composition as a candidate scaffold material was obtained by testing in solutions of increasing complexity [i.e., simulated body fluid (SBF, which contains ions similar to blood plasma) and Dulbecco's modified Eagle's medium (DMEM, which in addition to containing similar ionic concentrations as blood plasma also contains proteins common to blood)]. Furthermore, biomaterials are commonly tested in SBF, whereas DMEM is commonly used in cell culture media.

This article presents results that were obtained from reactivity testing in which S520 glass fibers were exposed to SBF and DMEM at 37°C for up to 20 days. Primary human osteoblast attachment to the S520 fiber surface, proliferation, nodule formation, and mineralization and the fiber tensile strength were also assessed.

MATERIALS AND METHODS

Before creating glass fiber, a precursor material was prepared from reagent grade Na_2CO_3 , K_2CO_3 , CaCO_3 , $\text{NH}_4\text{H}_2\text{PO}_4$, and SiO_2 to yield a glass of the nominal composition (in molar percentage) 52.0 SiO_2 , 20.9 Na_2O , 7.1 K_2O , 18.0 CaO , and 2.0 P_2O_5 . Fragments of this starting glass were then remelted in a platinum bushing, and fiber was drawn at a temperature between 1050 and 1100°C onto a rotating collection drum. An optical microscope was used to verify that the glass fiber possessed a consistent diameter of 20 μm .

Bioactive response

Bioactivity tests were conducted in triplicate by using an incubator set at 37°C and a rotational speed of 100 rpm. The bioactive response was monitored at 1, 5, 8, and 24 h and 2, 4, 10, and 20 days in both SBF and DMEM by using a fiber surface area to solution volume ratio (SA:V) of approximately 0.1 cm^2/mL . SBF, developed by Kokubo,¹¹ is a close

approximation of the ions composing human blood plasma. In addition, a set of samples was also tested in SBF using an SA:V ratio of approximately 0.05 cm^2/mL . When working with DMEM, the sample containers were sterilized with UV light, and all work was conducted in a laminar flow hood to prevent microbial contamination.

After the designated reaction time interval, the solution was decanted and stored under refrigeration for analysis by inductively coupled plasma (ICP) emission spectroscopy (ARL Fisons ICP Analyser 3580B). The reacted fibers were rinsed twice in acetone to arrest further reaction with the test solution and then dehydrated in a drying oven at 60°C. Scanning electron microscopy (SEM) was performed by using a Jeol T-220A, and energy dispersive X-ray spectroscopy (EDS) was performed by using a Jeol 200 with an Oxford Link attachment. Fourier transform infrared (FTIR) spectroscopic (Genesis II FTIR, Spectronic Unicam) analysis was conducted by using KBr pellets (1:100 weight ratio). Scans were taken between 1400 and 400 cm^{-1} .

Mechanical properties

The tensile strength of 20- μm S520 glass fibers was evaluated on the basis of the method prescribed in ASTM standard D-3379-75.¹² In brief, a section of fiber was glued (Araldite® epoxy, Bostik Ltd., UK) across the window of a mounting tab manufactured from heavy paper stock (230g sm, Ryman Ltd., UK). The dimensions of the window were 10 mm \times 20 mm (20-mm gauge length), and the overall dimensions of the tab were 25.4 mm \times 87 mm. After mounting, the sample was then placed in a drying oven at 60°C for at least 2 days to cure the epoxy. The crosshead displacement rate during tensile testing was 0.5 mm/min. The fiber strength was determined from the load at fracture and the fiber cross-sectional area. The Weibull modulus was also calculated from the 40 samples tested.

Preparation of fibers for cell culture

Fibers were cut to \sim 10 mm in length, sterilized by UV light for 30 min, and preincubated in DMEM culture medium for 24 h. Fibers were then rinsed in phosphate-buffered saline (PBS) and attached to 13-mm-diameter glass coverslips by using 4% agarose, applied at either end of the fibers.

Cell cultures

Primary human osteoblast cells were isolated as described previously¹³ from femoral heads after total hip replacement surgery. Bone fragments of \sim 3 mm \times 3 mm were removed. Fragments were washed several times in PBS to remove blood cells and debris with a final wash in culture medium. Fragments were then placed in tissue culture flasks in complete DMEM containing 10% fetal bovine serum (FBS) with

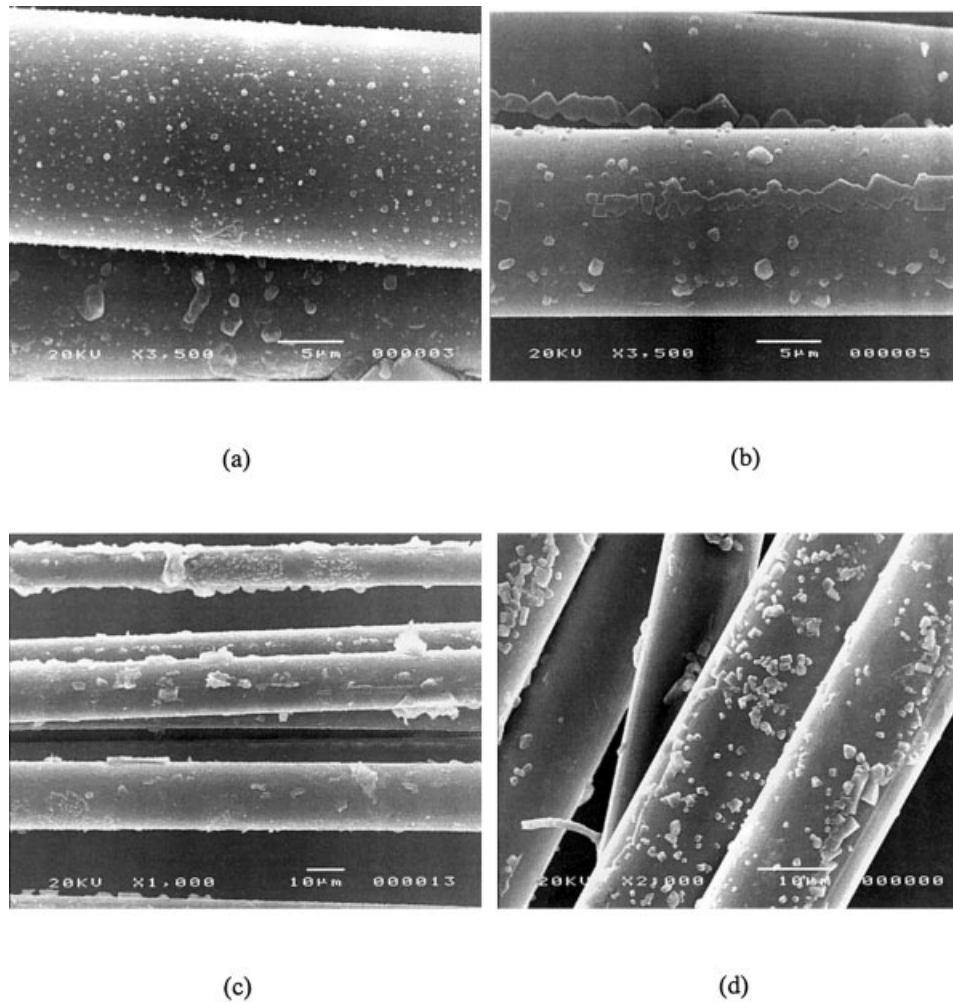


Figure 1. Scanning electron micrographs of S520 fiber surfaces after (a) 5 h, (b) 8 h, (c) 24 h, and (d) 48 h of immersion in SBF (0.1 SA:V). Hydroxyapatite is present as submicron-micron scale precipitates on the fiber surface.

1% glutamine, 2% penicillin/streptomycin, and 0.85 mM ascorbic acid. The fragments were incubated at 37°C in a humidified incubator with 5% CO₂. Medium was changed every 2 days and after ~4 weeks in culture, bone fragments were discarded and cells were harvested by using trypsin EDTA. Cells were used up to passage 6 and seeded onto materials at a density of 40,000 cells/cm².

SEM samples were prepared as follows. After culture for various periods, samples were washed twice in PBS and fixed in 3% glutaraldehyde in 0.1M phosphate buffer for 30 min at 4°C. Samples were then washed in phosphate buffer and postfixed in osmium tetroxide for 1 h at 4°C. Samples were washed again in phosphate buffer and dehydrated by using ethanol. After the final dehydration in 100% ethanol, samples were transferred to hexamethyldisilazane (HMDS), a chemical drying agent, for 5 mins. Samples were then rinsed in fresh HMDS and left in a fume hood to allow complete drying. Samples were sputter coated with gold and viewed under a Cambridge stereoscan S360 scanning electron microscope at 10 kV.

To determine culture mineralization, medium was supplemented with 10 mM β-glycerophosphate and 100 nM dexamethasone. Cells were cultured on the fibers as above

and then fixed with 70% ethanol, stained with alizarin red for 2 min, washed several times with distilled water, and viewed under a light microscope.

RESULTS

Bioactive response

The scanning electron micrographs shown in Figures 1(a) and (b) reveal that hydroxyapatite formed on the surface of S520 fibers after 5 h and 8 h immersion in SBF (0.1 SA:V), respectively. After 24–48 h in SBF, the amount of surface hydroxyapatite increased [Fig. 1(c) and (d)]. EDS analysis of the S520 fibers after 20 days in SBF (Fig. 2) revealed that the hydroxyapatite layer was well established, because only Ca and P were detected on the fiber surface. Figure 3 shows a backscattered electron image of the end of a S520 fiber immersed in SBF for 20 days. The contrast (Fig. 3)

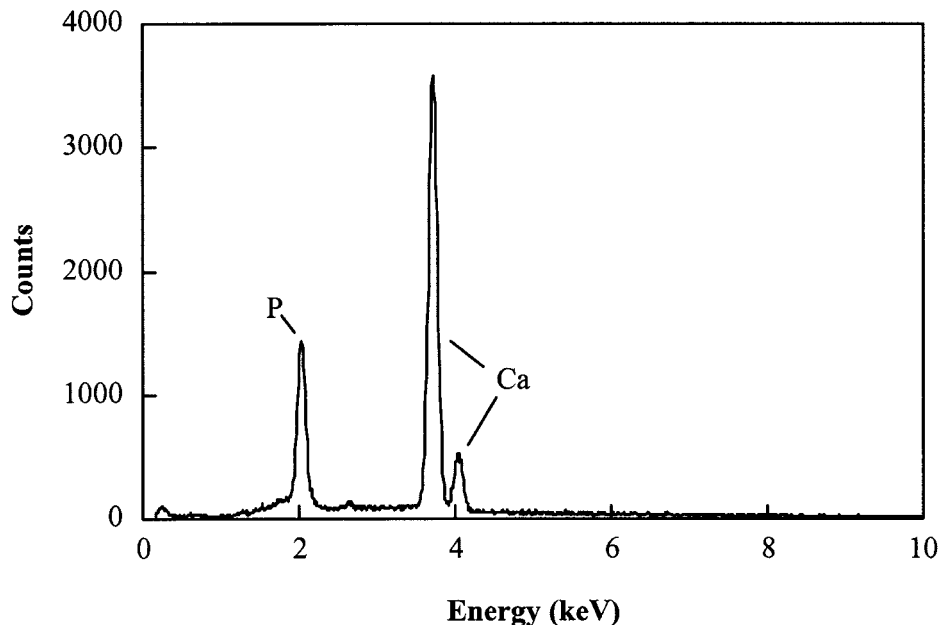


Figure 2. EDS spectra of S520 fiber surface after 20 days of immersion in SBF (0.1 SA:V).

between the fiber core and outer reaction layer ($\sim 5\text{-}\mu\text{m}$ thick) was indicative of a compositional difference.

The dissolution profile of S520 fibers in SBF (0.1 SA:V) is shown in Figure 4. Ca increased from ~ 100 to 175 ppm between 2 and 48 h and then decreased to ~ 100 ppm by 4 days and beyond. The P concentration was steady throughout the experiment at ~ 30 ppm. There was no pronounced deviation from the 5-h Si concentration (8 ppm), through 20 days.

In Figure 5 is shown the surface of S520 fibers after 20 days of soaking in DMEM. The fiber surface is covered by a continuous layer of hydroxyapatite glob-

ules $\sim 1\text{--}4\ \mu\text{m}$ in diameter. Closer examination of the globules reveals each was composed of smaller grains on the order of 50 nm. EDS spectra of the S520 fibers soaked for 20 days in DMEM revealed pronounced Ca and P peaks (Fig. 6) as well as other peaks corresponding to elements found in the parent glass.

The release profile of Si, Ca, and P into DMEM solution is shown in Figure 7. Through the first 4 days, the Ca concentration increased only slightly from ~ 80 to 90 ppm. The Ca concentration then decreased to ~ 50 ppm and 40 ppm after 10 and 20 days, respectively. Similarly, the phosphorous concentration (~ 30 ppm) underwent little deviation through 4 days before decreasing to ~ 10 ppm and 8 ppm after 10 and 20 days, respectively. The Si concentration was observed

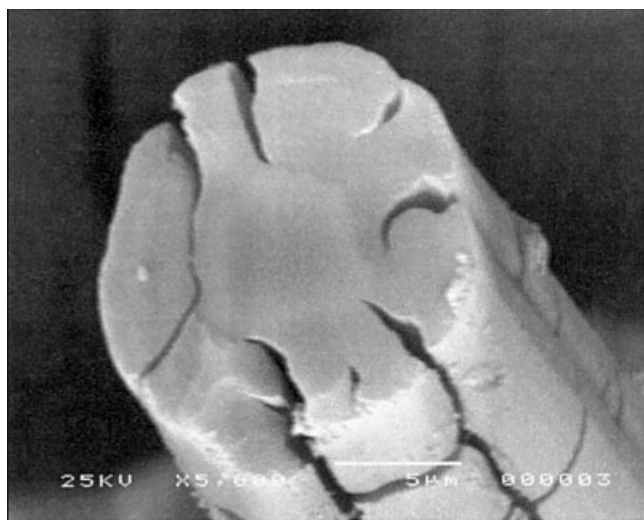


Figure 3. Backscattered SEM micrograph of S520 fiber after 20 days of immersion in SBF. The outer reaction layer ($\sim 5\ \mu\text{m}$) is contrasted with the inner fiber core.

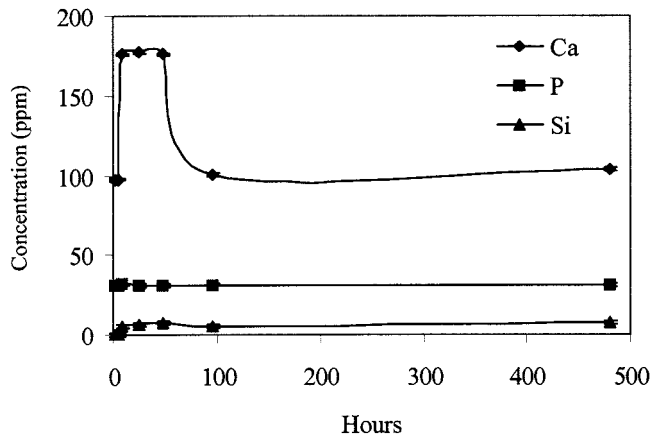


Figure 4. ICP data for S520 fibers immersed in SBF (0.1 SA:V). Errors bars ($n = 3$; 1 SD) were smaller than symbols used for each data point.

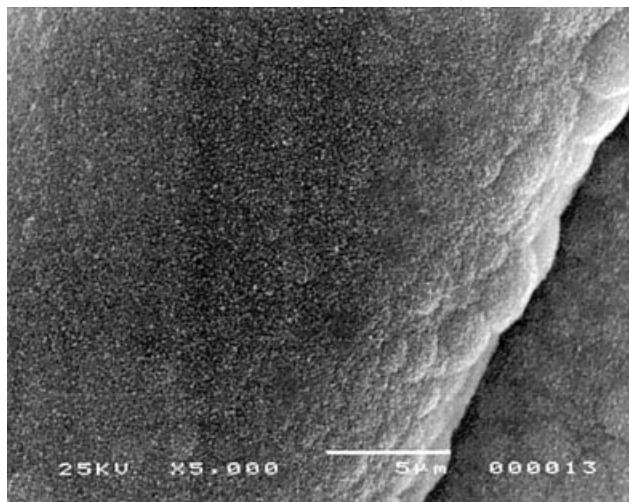


Figure 5. SEM micrographs of S520 fibers after 20 days of immersion in DMEM (0.1 SA:V).

to increase from $\sim 15\text{--}30\ \mu\text{g}/\text{mL}$ between 1 h and 2 days in solution. However, there was little change in the Si concentration between 2 and 7 days.

Because the SA:V ratio can influence the formation of hydroxyapatite surface layers,^{14–16} S520 fibers were additionally tested in SBF by using a second SA:V ratio, $0.05\ \text{cm}^2/\text{mL}$. After 2 days in solution, a continuous hydroxyapatite layer was clearly present on the fiber surface (Fig. 8). Formation of surface hydroxyapatite layers at 2 days and beyond is additionally revealed by examination of the FTIR spectra shown in Figure 9. After 2 days in solution, P-O bending peaks, indicative of the presence of hydroxyapatite, were located near $600\ \text{cm}^{-1}$

and $563\ \text{cm}^{-1}$. At 5 days and beyond, P-O peak splitting is evidence of a more thoroughly crystalline hydroxyapatite layer.¹⁷ Solution concentrations of Ca and P decreased significantly after 2 days (not shown), indicating further growth of the hydroxyapatite layer.

The average tensile strength of 20- μm -diameter S520 fibers (before SBF immersion) was $925 \pm 424\ \text{MPa}$ ($n = 40$). The Weibull strength distribution plot, shown in Fig. 10, yielded a Weibull modulus of 2.5, which is similar to other reported values for bioactive glass fibers.¹⁸

An initial study of the culture of primary human osteoblasts on the S520 fibers resulted in cell attachment, spreading, and proliferation. Figure 11 shows a low-power scanning electron micrograph of cells in a monolayer area after 7 days in culture, and Figure 12 shows a higher power monolayer area. Cells were elongated and mainly observed aligning along the long axes of the fibers. However, in some areas, cells were observed to wrap around individual fibers (Fig. 13). Osteoblasts were observed to also branch across fibers in close proximity to one another (Fig. 11). Osteoblast dorsal ruffles, cell projections, and lamellipodia were evident as shown in Figures 12, 13, and 14.

After supplementation of culture medium with dexamethasone and β -glycerophosphate, mineralized nodule formation was observed as shown by alizarin red staining in Figure 15. A darkly stained nodule is shown with fibers running through the center. Figure 16 shows negatively stained cells when cultured without such supplements.

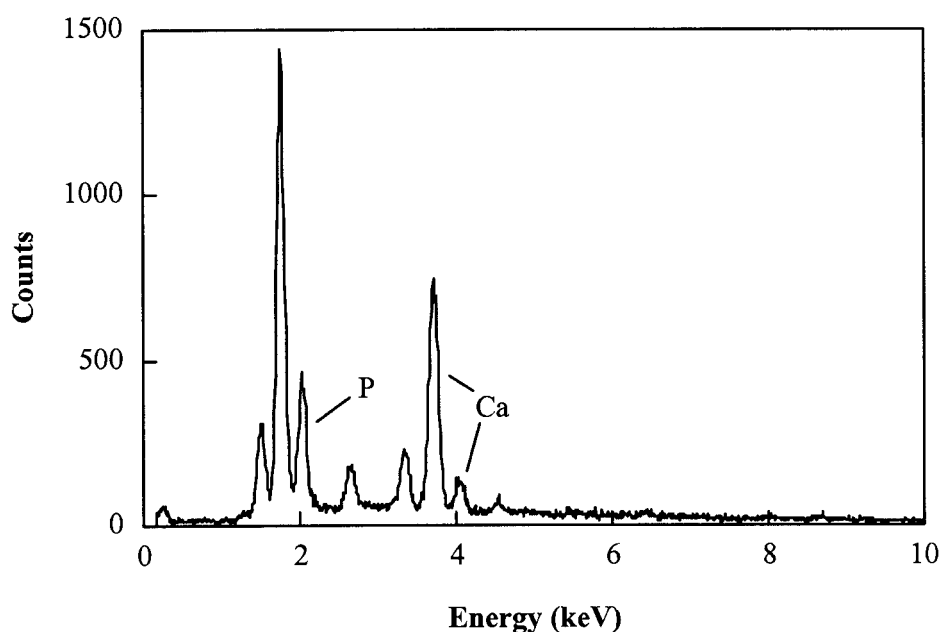


Figure 6. EDS spectrum of the S520 fiber surface after 20 days of immersion in DMEM (0.1 SA:V). The unlabeled peaks correspond to the other elements contained in the unreacted fiber.

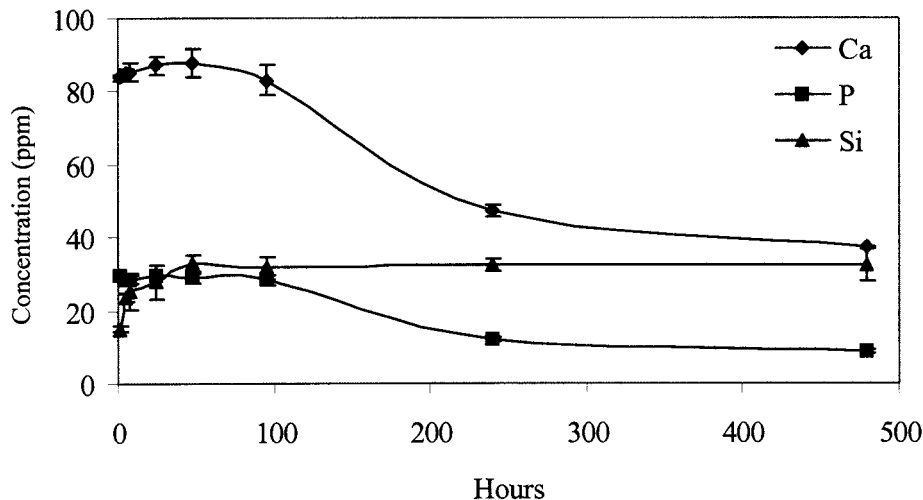


Figure 7. Concentrations Ca, P, and Si in DMEM test solutions (0.1 SA:V) as determined by ICP analysis. Errors bars ($n = 3$; 1 SD) were smaller than symbols used for some data points.

DISCUSSION

The bioactive response of novel S520 fibers (52.0 mol % SiO_2 , 20.9 Na_2O , 7.1 K_2O , 18.0 CaO , and 2.0 P_2O_5) *in vitro* in SBF and DMEM was characterized. Osteoblast attachment, proliferation, mineralized nodule formation, and fiber tensile strength were also assessed.

SEM micrographs revealed that hydroxyapatite globules formed on S520 fibers by 5 h in SBF (0.1 cm^2/mL), and this amount increased with immersion time. By 20 days (0.1 cm^2/mL SBF) the hydroxyapatite layer was continuous and preliminary analysis using EDS suggested that the reaction layer was relatively thick, because only Ca and P peaks were identified (Fig. 2). Further analysis by backscattered electron imaging revealed the thickness of the reaction layer formed after 20 days in SBF was 5 μm (Fig. 3). The

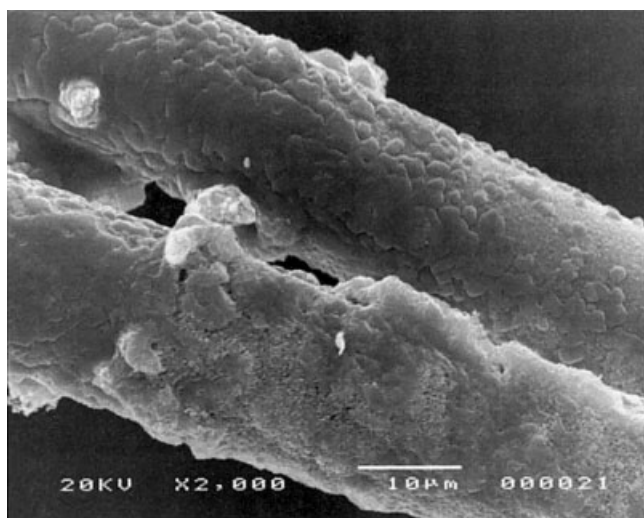


Figure 8. SEM micrograph of S520 fibers after 48 h in SBF (0.05 SA:V).

layer beneath the hydroxyapatite layer in bioactive glasses and glass-ceramics is often Si-rich.^{15,19–21}

SEM analysis clearly showed that a continuous reaction layer was produced by immersing S520 fibers in DMEM for 20 days. Subsequent EDS analysis of this layer revealed the presence of peaks other than Ca and P (e.g., Si). This finding indicated the reaction layer produced by DMEM immersion was not as thick ($< 5 \mu\text{m}$) as that caused by SBF immersion.

Previous work has shown that the SA:V ratio can

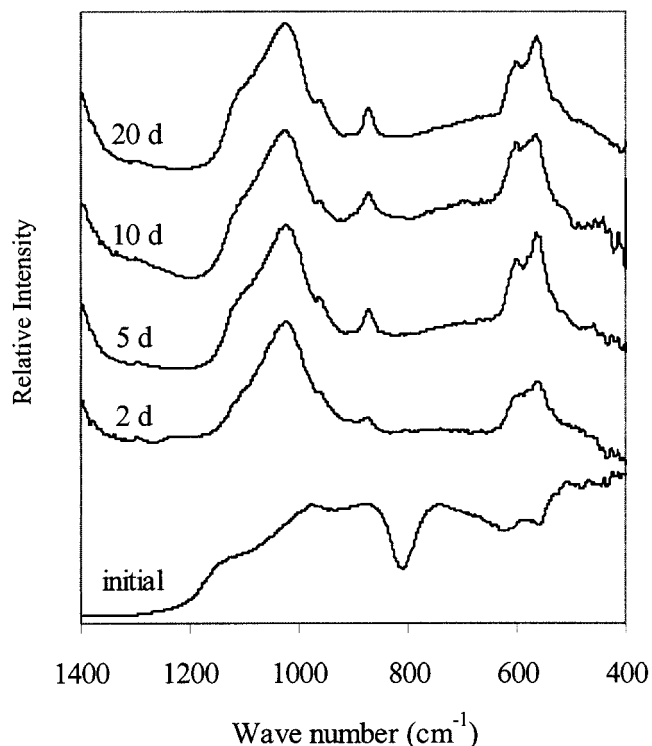


Figure 9. FTIR spectra of S520 fibers after immersion in SBF (0.05 SA:V).

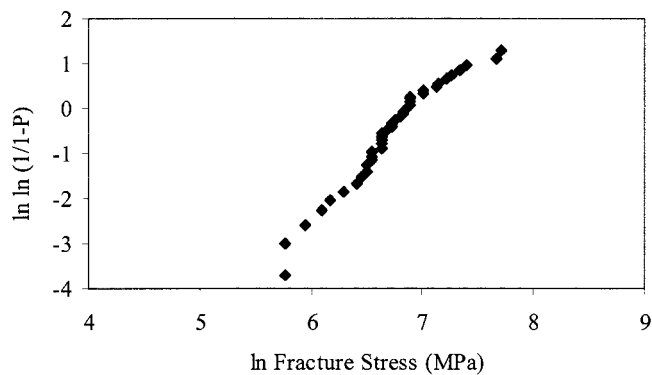


Figure 10. Weibull plot of S520 fibers loaded to failure in tension.

influence hydroxyapatite formation on the surface of a bioactive glass or glass-ceramic.¹⁴⁻¹⁶ Increasing the volume of SBF by a factor of 2 (0.05 SA:V) was observed to increase the rate of hydroxyapatite formation on S520 fibers, as a continuous reaction layer was observed after 2 days.

The results of the ICP analysis confirmed that the S520 glass fiber underwent dissolution when soaked in both SBF and DMEM solutions. Because of the high alkali ion content of the reaction media, it was not possible to monitor the cation exchange process (i.e., $H^+ \leftrightarrow Na^+, K^+$) which is thought to be the first mechanism accompanying silicate glass corrosion. However, the Si and Ca content of the leachate solutions provided a mean of monitoring the dissolution and reaction process.

Those tests conducted in SBF and DMEM using an SA:V ratio of 0.10 cm²/mL showed a rapid release of Si ions into solution in the first hours, after which time the Si concentration stabilized and remained essen-

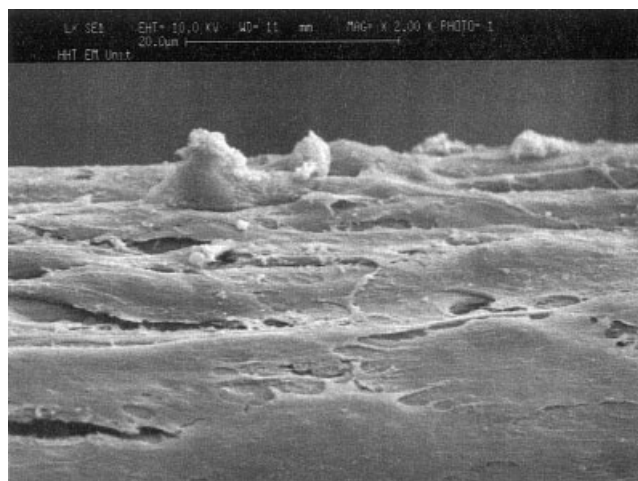


Figure 12. Scanning electron micrograph of HOBs cultured on fibers for 7 days. A monolayer of cells can be seen covering the fibers. Original magnification $\times 2000$.

tially constant up to 20 days. Similarly, Peltola et al.^{22,23} reported that hydroxyapatite formation followed the solution Si saturation point during the immersion of sol-gel derived silica fibers in SBF.

The Ca ion behavior was qualitatively similar for fiber dissolution in SBF and DMEM. An initial increase in concentration was observed, followed by a significant decrease that occurred between 2 and 4 days. However, the extent of dissolution of Ca in SBF was much higher, reaching a concentration of ~ 175 ppm, whereas Ca levels in the DMEM leachate showed only a moderate increase to ~ 90 ppm. The decline in Ca concentration over time in both solutions provided an indirect indication that a precipitation reaction had occurred. In the DMEM leachate, the P ion trendline was closely correlated to the decrease in

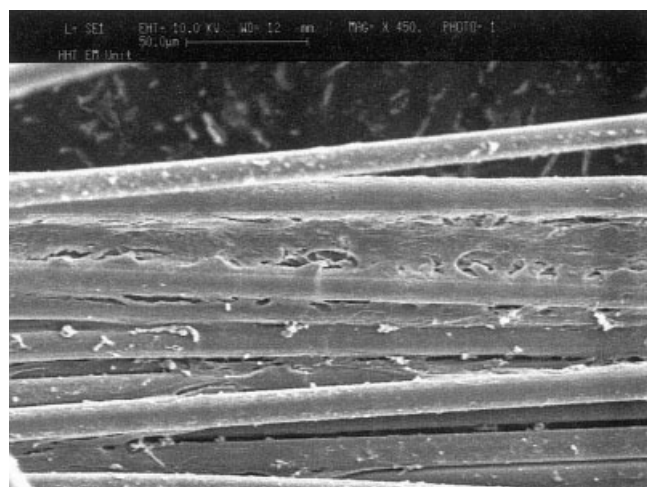


Figure 11. Scanning electron micrograph of human osteoblasts (HOBs) cultured on fibers for 7 days. At this low power the arrangement of fibers and cells can be seen. Original magnification $\times 450$.

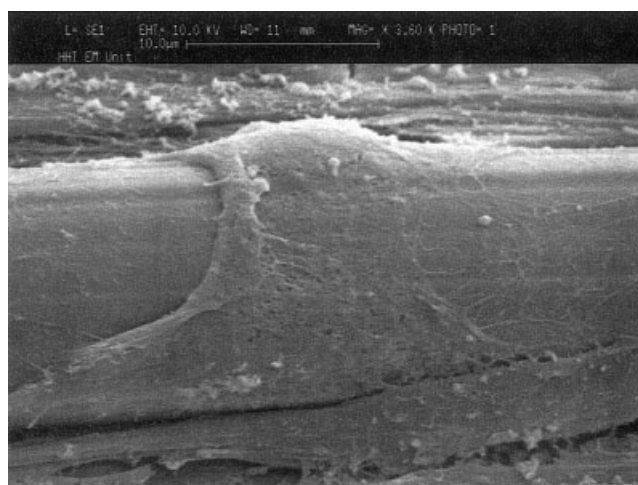


Figure 13. Scanning electron micrograph of HOBs cultured on fibers for 7 days. A cell can be seen wrapped around a single fiber. Original magnification $\times 3600$.

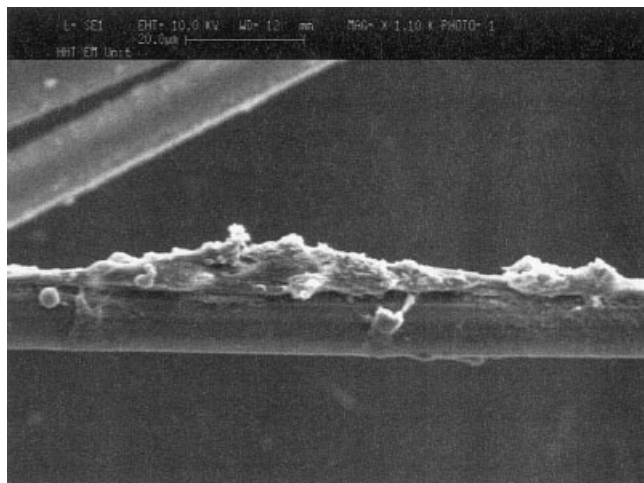


Figure 14. Scanning electron micrograph of HOBs cultured on fibers for 7 days. A cluster of cells can be seen attaching to a single fiber. Original magnification $\times 1100$.

Ca concentration, suggesting that a calcium phosphate compound was precipitating out of solution.

The pronounced increase in Ca concentrations during the first hours for fibers soaked in SBF suggests that a second phase may have precipitated, allowing for the Ca concentration (which was already supersaturated) to rise. Further testing may be necessary to elucidate the role of soluble Si on hydroxyapatite formation. Peltola et al.^{22,23} observed that the amount of Si released from sol-gel-derived silica fibers into SBF did not influence the formation of the hydroxyapatite surface layers *in vitro*. However, it has been shown that soluble Si is important for bone formation *in vivo*.²⁴

The ionic concentrations resulting from S520 fiber immersion in DMEM were, after the first hour (Si 15.1 ± 0.8 , Ca 83.8 ± 1.0 , and P 29.7 ± 0.2 ppm, respectively) similar to those concentrations previously determined to stimulate gene expression in osteoblasts *in vitro* (Si 16.5 ± 3.5 , Ca 88.3 ± 4.6 , and 30.4 ± 1.2 ppm, respectively).⁹ Xynos et al.⁹ obtained a solution of the aforementioned specific Si, Ca, and P concentrations by soaking particulate 45S5 bioactive glass in DMEM for 48 h. Treatment of human osteoblasts with this solution caused upregulation of many genes and proteins, including CD44 antigen hemopoietic form precursor (increase by a factor of $7\times$); MAP kinase-activated protein kinase 2 (MAPKAP kinase 2) ($6\times$); integrin $\beta 1$, fibronectin receptor β -subunit ($6\times$); RCL growth-related c-myc-responsive gene ($5\times$); defender against cell death 1 (DAD-1) ($4.5\times$); heat shock cognate 71-kDa protein ($4.5\times$); and calpain, calcium-dependent protease small subunit ($4.1\times$). In addition, there were 14 genes upregulated in the range of 3.0 – $3.6\times$ and 36 in the range 2.0 – $2.9\times$.

The FTIR spectra shown in Figure 9 for S520 fibers soaked in 0.05 SA:V SBF indicate a splitting of the P-O bending peak with increasing time. This indicates that the reaction layer is attaining a higher degree of crystallinity with increasing immersion time.¹⁷ Similarly, Orefice et al.²⁵ reported amorphous calcium phosphate formation on 77S sol-gel-derived fibers after 20 h in SBF before crystalline dual peaks formation after 48 h.

The tensile strength of S520 fibers ($20\text{-}\mu\text{m}$ diameter), 925 ± 424 MPa, is sufficient for use as a tissue scaffold material. The strength of bioactive 45S5 fibers was reported by DeDeigo et al.¹⁸ to be 93 ± 38 MPa (165 –



Figure 15. Light micrograph of HOBs cultured on the fibers for 14 days with 10 mM β -glycerophosphate and 100 nM dexamethasone, stained with alizarin red. A large positively stained nodule is shown. Original magnification $\times 200$. [Color figure can be viewed in the online issue, which is available at www.interscience.wiley.com.]

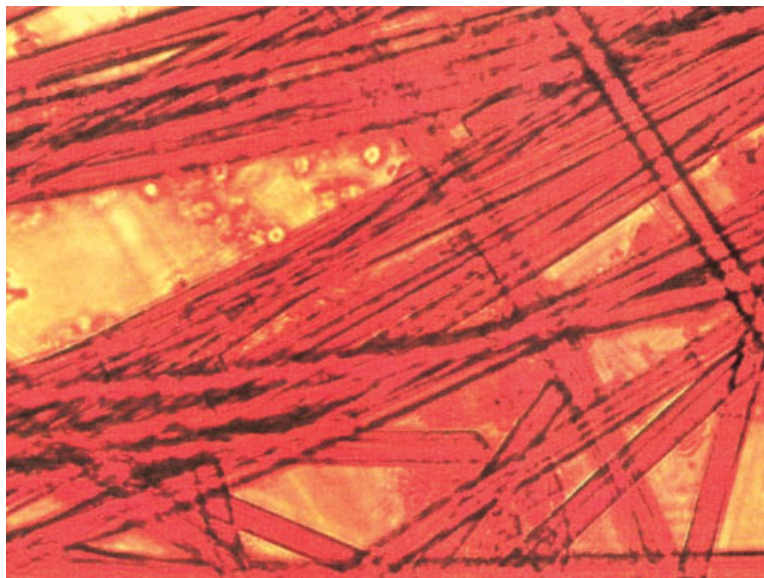


Figure 16. Light micrograph of HOBs cultured on the fibers for 14 days without β -glycerophosphate or dexamethasone, stained with alizarin red. Cells are negatively stained. Original magnification $\times 200$. [Color figure can be viewed in the online issue, which is available at www.interscience.wiley.com.]

220- μm diameter) and 82 ± 23 MPa (250–310- μm diameter). These pronounced tensile strength differences between the SiO_2 -based bioactive fibers are as expected, because a decreasing fiber diameter leads to an increase in strength because the distribution of critical sized flaws will also be smaller, on average. The Weibull modulus, an indication of the stress distribution, was 2.5 for the S520 fibers. Similar values, 3.0 and 3.5, were reported for 165–220- μm and 250–310- μm diameter 45S5 bioactive glass fibers, respectively.¹⁸

The initial findings of osteoblast responses to S520 fibers were encouraging. Osteoblasts were observed to attach, proliferate, and form mineralized nodules on the fibers in the presence of dexamethasone and β -glycerophosphate. Osteoblast attachment and proliferation are required for the development of the mature osteoblast phenotype and, therefore, formation of mineralized nodules. Inclusion of mineralization supplements, such as dexamethasone and β -glycerophosphate, are widely used to promote mineralization of osteoblast cultures^{26–29} and to demonstrate the ability of the cells to mineralize in specific culture conditions. Mineralization of cultures in this *in vitro* study shows potential for new bone formation to occur *in vivo*. Further studies will include gene expression analysis.

CONCLUSIONS

SEM, EDS, ICP, and FTIR were used to determine that S520 glass fibers, a composition amenable to fiber formation, were bioactive in SBF and DMEM. EDS and

SEM analysis suggested that the reaction layer formed on the surface was less thick for DMEM than for SBF immersion. In addition, a lower SA:V ratio was observed to lead to a decrease in the time required for the formation of a continuous surface hydroxyapatite layer in SBF. Si, Ca, and P release from DMEM solutions was found to closely coincide with the solution ionic concentrations of bioactive glass dissolution products previously found to stimulate gene transcription in primary human osteoblasts. The fiber tensile strength was 925 MPa. Preliminary osteoblast culture studies on the S520 fiber surface were promising, showing proliferation, nodule formation, and mineralization.

The authors thank Dr. Tim Ryder and Mrs. Margaret Moberley from The Electron Microscopy Unit, Department of Histopathology, Charing Cross Hospital, London, for assistance with scanning electron microscopy of the cell cultures. The authors also thank Mr. Barry Coles of Imperial College for assistance with ICP analysis. Partial financial support of the following organizations is acknowledged: USBiomaterials Corp., (Alachua, FL), the March of Dimes, the Alcoa Foundation, the United Kingdom Medical Research Council, and the Engineering and Physical Sciences Research Council.

References

1. Sepulveda P, Jones JR, Hench LL. Bioactive sol-gel foams for tissue repair. *J Biomed Mater Res* 2002;59:340–348.
2. Hutmacher DW. Scaffolds in tissue engineering bone and cartilage. *Biomaterials* 2000;21:2529–2543.

3. Domingues RZ, Clark AE, Brennan AB. A sol-gel derived bioactive fibrous mesh. *J Biomed Mater Res* 2001;55:468-474.
4. Hench LL, Splinter RJ, Allen WC, Greenlee TK. Bonding mechanisms at the interface of ceramic prosthetic materials. *J Biomed Mater Res Symposium* 1971;2:117-141.
5. Kokubo T, Kushitani H, Sakka S, Kitsugi T, Yamamuro T. Solutions able to reproduce *in vivo* surface-structure changes in bioactive glass-ceramic A-W. *J Biomed Mater Res* 1990;24:721-734.
6. Brink M, Turunen T, Happonen R-P, Yli-Urpo A. Compositional dependence of bioactivity of glasses in the system $\text{Na}_2\text{O}-\text{K}_2\text{O}-\text{MgO}-\text{CaO}-\text{B}_2\text{O}_3-\text{P}_2\text{O}_5-\text{SiO}_2$. *J Biomed Mater Res* 1997;37:114-121.
7. Hench LL. Bioactive ceramics: theory and clinical applications. In: Andersson ÖH, Happonen R-P, Yli-Urpo A, editors. *Bioceramics 7*. Oxford: Pergamon; 1994. p 3-14.
8. Loty C, Sautier J-M, Boulekbache H, Kokubo T, Kim H-M, Forest N. *In vitro* bone formation on a bone-like apatite layer prepared by a biomimetic process on a bioactive glass-ceramic. *J Biomed Mater Res* 2000;49:423-434.
9. Xynos ID, Edgar AJ, Buttery LDK, Hench LL, Polak JM. Gene transcription profiling of human osteoblasts following treatment with ionic products of Bioglass 45S5 dissolution. *J Biomed Mater Res* 2001;55:151-157.
10. Clapp PI, M.S. thesis, New York: Alfred University; 2001.
11. Kokubo T. A/W glass-ceramic: processing and properties. In: Hench LL, Wilson J, editors. *An introduction to bioceramics*. Singapore: World Scientific; 1993 p. 75-87.
12. ASTM Standard. Test method for tensile strength and Young's modulus for high modulus single filament materials: D 3379-75.
13. Wergedal JE, Baylink DJ. Characterization of cells isolated from human bone. *Proceedings of the Society for Experimental Biology and Medicine* 1984;176:60-69.
14. Greenspan DC, Zhong JP, LaTorre GP. Effect of surface area to volume ratio on *in vitro* surface reactions of bioactive glass particulates. In: Andersson ÖH, Happonen R-P, Yli-Urpo A, editors. *Bioceramics 7*. Oxford: Pergamon; 1994. p 55-60.
15. Clupper DC, Mecholsky JJ Jr, LaTorre GP, Greenspan DC. Sintering temperature effects on the *in vitro* bioactive response of tape cast and sintered bioactive glass-ceramic in Tris buffer. *J Biomed Mater Res* 2001;57:532-540.
16. Jones JR, Sepulveda P, Hench LL. Dose dependent behavior of bioactive glass dissolution. *J Biomed Mater Res (Appl Biomater)* 2001;58:720-726.
17. Asplin JR, Mandel NS, Coe FL. Evidence for calcium phosphate supersaturation in the loop of Henle. *Am J Physiol* 1996;270:F604-F613.
18. De Diego MA, Coleman NJ, Hench LL. Tensile properties of bioactive fibers for tissue engineering applications. *J Biomed Mater Res* 2000;53:199-203.
19. Ylanen H, Karlsson KH, Itala A, Aro HT. Effect of immersion in SBF on porous bioactive bodies made by sintering bioactive glass microspheres. *J Non-Cryst Sol* 2000;275:107-115.
20. Clark AE Jr, Pantano CG Jr, Hench LL. Auger spectroscopic analysis of Bioglass corrosion films. *J Am Ceram Soc* 1976;59:37-39.
21. Ohtsuki C, Kokubo T, Yamamuro T. Mechanism of apatite formation on $\text{CaO}-\text{SiO}_2-\text{P}_2\text{O}_5$ glasses in a simulated body fluid. *J Non-Cryst Sol* 1992;143:84-92.
22. Peltola T, Jokinen M, Veittola S, Rahiala H, Yli-Urpo A. Influence of sol and stage of spinnability on *in vitro* bioactivity and dissolution of sol-gel-derived SiO_2 fibers. *Biomaterials* 2001;22:589-598.
23. Peltola T, Jokinen M, Veittola S, Simola J, Yli-Urpo A. *In vitro* bioactivity and structural features of mildly heat-treated sol-gel-derived silica fibres. *J Biomed Mater Res* 2001;54:579-590.
24. Carlisle EM. Silicon: a requirement in bone formation independent of vitamin D1. *Calcif Tiss Int* 1981;33:27-34.
25. Orefice RL, Hench LL, Clark AE, Brennan AB. Novel sol-gel bioactive fibers. *J Biomed Mater Res* 2001;55:460-467.
26. Coelho MJ, Fernandes MH. Human bone cell cultures in biocompatibility testing. Part II Effect of ascorbic acid, β -glycerophosphate and dexamethasone on osteoblastic differentiation. *Biomaterials* 2000;21:1095-1102.
27. Abe Y, Aida Y, Abe T, Hirofuji T, Anan H, Maeda K. Development of mineralised nodules in fetal rat mandibular osteogenic precursor cells: requirement for dexamethasone but not for β -glycerophosphate. *Calcif Tissue Int* 2000;66:66-69.
28. Ecarot-Charrier B, Glorieux FH, van der Rest M, Pereira G. Osteoblasts isolated from mouse calvaria initiate matrix mineralisation in culture. *J Cell Biol* 1983;96:639-643.
29. Fratzl-Zelman N, Fratzl P, Horandner H, Grabner B, Varga F, Ellinger A, Klaushofer K. Matrix mineralisation in MC3T3-E1 cell cultures initiated by β -glycerophosphate pulse. *Bone* 1998;23:511-520.